IAI Journals.ASM.org

Agglutinating Secretory IgA Preserves Intestinal Epithelial Cell Integrity during Apical Infection by *Shigella flexneri*

Amandine Mathias, Stéphanie Longet, Blaise Corthésy

R&D Laboratory of the Division of Immunology and Allergy, Centre Hospitalier Universitaire Vaudois, Lausanne, Switzerland

***Shigella flexneri*, by invading intestinal epithelial cells (IECs) and inducing inflammatory responses of the colonic mucosa, causes bacillary dysentery. Although M cells overlying Peyer's patches are commonly considered the primary site of entry of *S. flexneri*, indirect evidence suggests that bacteria can also use IECs as a portal of entry to the lamina propria. Passive delivery of secretory IgA (SIgA), the major immunoglobulin secreted at mucosal surfaces, has been shown to protect rabbits from experimental shigellosis, but no information exists as to its molecular role in maintaining luminal epithelial integrity. We have established that the interaction of virulent *S. flexneri* with the apical pole of a model intestinal epithelium consisting of polarized Caco-2 cell monolayers resulted in the progressive disruption of the tight junction network and actin depolymerization, eventually resulting in cell death. The lipopolysaccharide (LPS)-specific agglutinating SIgAC5 monoclonal antibody (MAb), but not monomeric IgAC5 or IgGC20 MAbs of the same specificity, achieved protective functions through combined mechanisms, including limitation of the interaction between *S. flexneri* and epithelial cells, maintenance of the tight junction seal, preservation of the cell morphology, reduction of NF-κB nuclear translocation, and inhibition of proinflammatory mediator secretion. Our results add to the understanding of the function of SIgA-mediated immune exclusion by identifying a mode of action whereby the formation of immune complexes translates into maintenance of the integrity of epithelial cells lining the mucosa. This novel mechanism of protection mediated by SIgA is important to extend the arsenal of effective strategies to fight against *S. flexneri* mucosal invasion.**

Shigella flexneri, the causative agent of bacillary dysentery, invades nonphagocytic cells through the type III secretion system (T3SS), which delivers bacterial effectors that trigger severe inflammatory reactions, eventually leading to epithelium destruction (1). Successive events, including Peyer's patch (PP) M cell-mediated entry (2), apoptosis of infected macrophages (3), and recruitment of polymorphonuclear cells that further amplify local damage (4), promote the access of *S. flexneri* to the basolateral surface of epithelial cells. Subversion of host cell architecture through the injection of effector proteins promotes the cell-to-cell propagation of infection, a process accompanied by the epithelial production of proinflammatory mediators (5). *In vitro* models using enterocyte-derived monolayers partially or not differentiated have led to the most-favored conclusion, that *S. flexneri* invades intestinal epithelial cell (IEC) monolayers exclusively from the basolateral pole (6). However, both *in vitro* and *in vivo* models have identified the effectiveness of epithelial infection from the apical brush border, arguing for an alternative site of entry for the bacterium besides PPs (7–9). Although rapid remodeling of tight junction organization by *S. flexneri* has been documented (9), the more long-term effect on IEC responsiveness is in need of investigation.

Both innate and acquired types of immune responses have been implicated in combating *S. flexneri* infection, reflecting the complexity of the protection processes (10–12). In the gastrointestinal tract, the local adaptive humoral response is essentially mediated by secretory IgA (SIgA), the main immunoglobulin found at the mucosal surface. The protective function of specific SIgA against *S. flexneri* has been described *in vivo* using rabbit ileal loops, as well as in samples from infected patients (12–17), and relies on immune exclusion, preventing epithelial damage. However, how the protective role of the antibody (Ab) is relayed to IEC wellness and, thus, its essential barrier function is not known. Recently published data demonstrated a transient suppression of the T3SS when the bacteria were incubated with the lipopolysaccharide (LPS)-specific monoclonal antibody (MAb) IgAC5 (18). This feature and the role of T3SS in initial infectious processes prompted us to examine the mechanisms by which SIgA-based protection can be mediated at the intestinal luminal surface. Polarized Caco-2 cell monolayers, serving as a mimic of the intestinal epithelium for controlling the passage of antigens and potentially harmful microorganisms, were infected with bacteria either alone or in complexes with LPS-specific SIgAC5, monomeric IgAC5, IgGC20, and the *Salmonella enterica* serovar Typhimurium-specific SIgASal4 as a nonspecific control. We found that apical exposure of Caco-2 cells to *S. flexneri* triggered progressive cytoskeletal and tight junction disorganization that favors bacterial diffusion, a chronologic process that was specifically delayed by the agglutination properties of the anti-LPS SIgAC5 MAb. SIgA-mediated neutralization of *S. flexneri* interfered with IEC responsiveness, as mapped by altered NF-κB nuclear translocation and a drop in cytokine/chemokine release. As such preventive actions did not occur in the presence of monomeric IgAC5, IgGC20, or SIgASal4, our study demonstrates the specific functions of SIgAC5 in limiting bacterial binding, maintaining epithelial cell integrity, preventing cellular dissemination of the bacterium, and reducing

Received 13 March 2013 **Returned for modification** 27 April 2013
Accepted 2 June 2013
Published ahead of print 10 June 2013
Editor: S. M. Payne
Address correspondence to Blaise Corthésy, blaise.corthesy@chuv.ch.

doi:10.1128/IAI.00303-13

subsequent activation of proinflammatory messengers, a series of events involved in *S. flexneri* infection from the apical epithelial surface.

MATERIALS AND METHODS

Caco-2 cell culture and transepithelial electrical resistance measurements. The human colonic adenocarcinoma epithelial Caco-2 cell line (American Type Tissue Collection) was seeded on polyester Snapwell filters (diameter, 12 mm; pore size, 0.4 μm; Corning Costar) as described previously (19). The cells were grown in complete Dulbecco's modified Eagle's medium DMEM (C-DMEM) supplemented with 10% fetal calf serum (FCS; Sigma), 1% nonessential amino acids (Gibco), 1% glutamine, 10 mM HEPES (Invitrogen), 0.1% transferrin (Invitrogen), and 1% streptomycin-penicillin (Sigma). The integrity of the polarized Caco-2 cell monolayers was checked by measuring the transepithelial electrical resistance (TER) with a Millicell electrical resistance system (ERS) (Millipore). The TER values of well-differentiated monolayers ranged from 450 to 550 Ω/cm^2. A drop in TER values below 250 Ω/cm^2 is indicative of damaged cellular integrity.

Microorganisms and growth conditions. The serotype 5a, LPS-producing virulent *S. flexneri* strain M90T constitutively expressing green fluorescent protein (GFP) (20) was cultured and quantified as described previously (21).

Cell lines and protein production. Mouse IgAC5 (22) and IgGC20 (23) MAbs that are specific for *S. flexneri* serotype 5a LPS and mouse IgASal4 (24) MAb that is specific for *Salmonella* Typhimurium surface carbohydrates were cultured as described previously (25). Polymeric and monomeric forms of the IgAC5 Ab were separated by size exclusion chromatography (25). The mouse secretory component obtained from hybridoma 2H2 (26) was combined with equimolar amounts of polymeric IgA (pIgA) MAbs in phosphate-buffered saline (PBS) at room temperature (RT) to generate SIgAC5 and SIgASal4, respectively (27).

Antibody association to bacteria. Amounts of 2×10^7 bacteria were mixed with 10 μg of SIgAC5 or SIgASal4 or 2 μg of IgGC20 or monomeric IgAC5 in a final volume of 500 μl of PBS and incubated for 1 h at RT under gentle agitation. The immune complexes were washed 3 times in PBS and resuspended in plain DMEM (P-DMEM) complemented with 10 mM HEPES for analysis of MAb-mediated agglutination or bacterial growth or to infect polarized Caco-2 cell monolayers (multiplicity of infection [MOI] = 20).

The stability of immune complexes was visualized at 1 h and after overnight incubation with biotinylated goat anti-mouse Ig α chain (1/10; Cappel) or biotinylated goat anti-mouse Ig γ chain (1/50, Invitrogen), followed by cyanine 5 (Cy5)-conjugated streptavidin (1/500; GE HealthCare). Labeled immune complexes were laid onto glass slides (Thermo Scientific), fixed in 2% paraformaldehyde in PBS for 25 min at RT, mounted in Vectashield solution (Vector Laboratories), and visualized using a Zeiss LSM 710 Meta confocal microscope (Carl Zeiss, Germany) equipped with a 63× objective (imaging facility, UNI-Lausanne). Images were processed with Zeiss ZEN 2009 light software.

To measure the direct impact of the MAbs on bacterial growth, suspensions of bacteria alone or associated in immune complexes were evaluated by measuring optical density (OD; 1 OD unit at 600 nm corresponds to 1×10^8 *S. flexneri*) 3 and 6 h after the formation of immune complexes and after overnight incubation in solution at 37°C. As agglutination resulted in sedimentation of bacteria, OD was measured after resuspension. We favored this method instead of plating because agglutination by SIgAC5 might have led to a bias due to overlapping colonies emanating from immune complexes containing several bacteria.

Exposure of Caco-2 cells to bacteria. One hour before the use of polarized Caco-2 cell monolayers, C-DMEM was replaced by P-DMEM in both the apical and basolateral compartments. The apical medium was then replaced by 500 μl of bacterial suspensions (2×10^7 bacteria, MOI = 20) as such or in the form of immune complexes. TER values were measured at selected time points from the beginning of the infection onward. In selected experiments, Caco-2 cells were treated or not with 50 μg/ml gentamicin for 30 min, washed in sterile PBS, and incubated for 3 min in lysis buffer (10 mM Tris-HCl [pH 7], 0.2% Nonidet P-40, 50 mM NaCl, 2 mM EDTA [pH 8]). Lysates were seeded on LB agar plates containing 50 μg/ml of ampicillin, and CFU were determined after overnight incubation at 37°C.

Laser scanning confocal microscopy (LSCM) observation of Caco-2 cell monolayers. Infected polarized Caco-2 cell monolayers grown in Snapwell filters were washed with PBS prior to fixation overnight with 5 ml of 4% paraformaldehyde at 4°C. After washing with PBS, nonspecific binding sites on filters were blocked with PBS containing 5% FCS and 0.2% Triton X-100 (PBS-T) for 30 min at RT. All Abs were diluted in PBS-T. Filters were incubated with rabbit anti-human ZO-1 antibody (1/200, Invitrogen) for 2 h at RT and washed in PBS, followed by incubation with goat anti-rabbit IgG conjugated with Alexa Fluor 647 (1/100; Invitrogen) for 90 min at RT. When assessed, phalloidin associated with Fluoprobes 547H (1/200; Interchim) was incubated concomitantly with the secondary Ab. To visualize cells, filters were finally incubated with 100 ng/ml of 4′,6′-diamidino-2-phenylindole (DAPI) in PBS (Invitrogen) for 30 min. Filters were cut out of their holders and mounted in Vectashield solution for observation with a Zeiss LSM 710 Meta confocal microscope (Carl Zeiss) equipped with either a 10× or a 40× objective. Images were processed with Zeiss ZEN 2009 light software.

Quantification of the number of invasion foci and the overall infection area. The observation of whole filters was carried out with the 10× objective using Zeiss ZEN 2009 light software. The number of invasion foci and the sum of infected areas were automatically determined with the particle analysis tool of ImageJ software in the channel detecting GFP-expressing bacteria. When the area affected by the bacteria reached a macroscopically observable loss of the polarized monolayers, the remaining areas covered by adherent cells were determined with the differential interference contrast (DIC) channel as a substitute for the channel measuring green fluorescence.

ELISA. Human CCL3, tumor necrosis factor alpha (TNF-α), and CXCL8 in the basolateral compartment of polarized Caco-2 cell monolayers were quantitated by enzyme-linked immunosorbent assay (ELISA) with commercial kits (BD Biosciences and R&D Systems).

Analysis of NF-κB nuclear translocation. Preparation of Caco-2 cell small-scale nuclear extracts was carried out as described previously (28). Members of the NF-κB family present in the nuclei from Caco-2 cells were identified by immunoblotting (28) with rabbit antiserum directed against the p50 or p65 subunit (1/500; Santa Cruz Biotechnology) followed by horseradish peroxidase (HRP)-conjugated goat anti-rabbit IgG (1/5,000; Sigma-Aldrich) and using the chemiluminescence UptiLight kit (Interchim).

Statistical analysis. The results are given as means + standard errors of the means (SEM). Two-tailed nonparametric Mann-Whitney *U*-test analysis was performed using GraphPad Prism 5 software. Differences were considered significant when P values of <0.05 were obtained.

RESULTS

Only specific anti-LPS SIgAC5 interferes with the apical infection pattern of *Shigella* in polarized Caco-2 cell monolayers. Polarized Caco-2 cell monolayers were apically exposed to virulent *S. flexneri* strain M90T alone or in complexes with specific anti-LPS SIgAC5, IgGC20, monomeric IgAC5, or irrelevant SIgASal4 MAbs. Combined measurements of TER values and numeration of bacteria present in cell lysates were used to assess the integrity of the IEC monolayers and the degree of infection, respectively. With the notable exception of incubation with M90T-SIgAC5, overnight apical infection with M90T alone or in combination with other various MAbs triggered a 70% reduction in TER values (200 Ω/cm^2), indicative of a drastic alteration of the Caco-2 monolayer (Fig. 1A). The presence of the invasion plasmid antigens in M90T

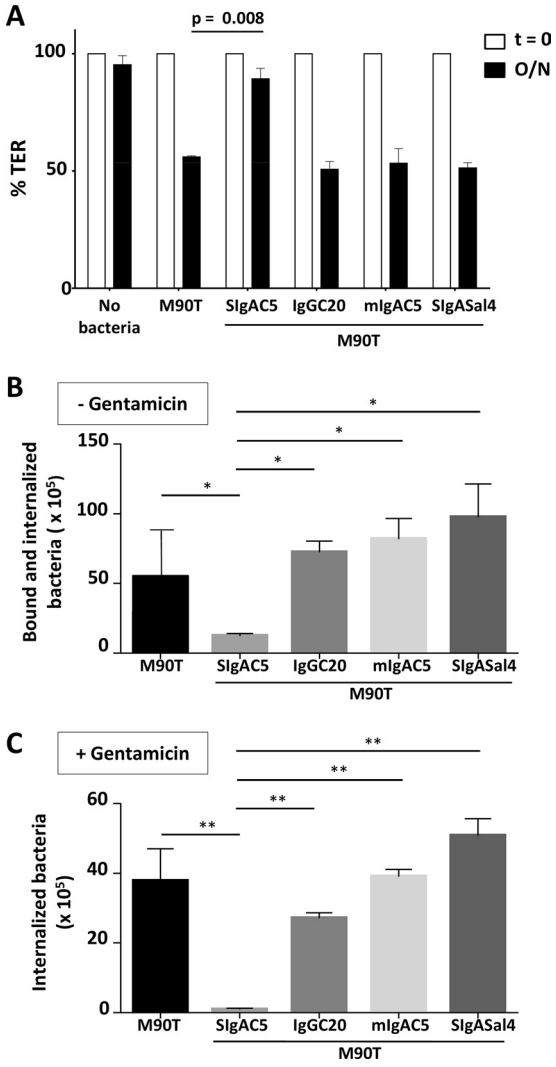

FIG 1 SIgAC5 maintains the integrity of polarized Caco-2 cell monolayers by retarding infection by virulent *S. flexneri*. (A) TER changes of intestinal Caco-2 cell monolayers exposed overnight (O/N) to *S. flexneri* M90T alone or in immune complexes with anti-LPS SIgAC5, IgGC20, or monomeric IgAC5 (mIgAC5) and irrelevant SIgASal4 as a control were monitored. Data correspond to one representative experiment ($n = 3$) for each tested condition performed in triplicates. TER of noninfected Caco-2 cell monolayers was arbitrarily set at 100%. (B, C) Adhesion/internalization of *S. flexneri* M90T alone or associated with SIgAC5, IgGC20, mIgAC5, and SIgASal4 to polarized Caco-2 cell monolayers as determined after overnight incubation in the absence (B) or presence (C) of gentamicin treatment for 30 min. Data are expressed on a per-filter basis and correspond to one representative experiment ($n = 3$) for each tested condition performed in triplicates. Mean values + SEM are shown. Statistically significant differences calculated by comparison with M90T-SIgAC5 are indicated above the columns as follows: *, $P \leq 0.05$; **, $P \leq 0.01$.

was required for IEC infection, as incubation with the avirulent *S. flexneri* mutant BS176 (29) did not affect TER (not shown). Because IgGC20 or monomeric IgAC5 with the same specificity as SIgAC5 could not compensate for the TER drop, this suggests that both the isotype and the molecular form of the Ab were essential to its protective function *in vitro*. However, antigen binding specificity was required, as SIgASal4 recognizing *Salmonella* Typhimurium surface carbohydrates did not prevent TER drop either; this further indicated that secretory component present in SIgAC5 was not involved in the preservation of Caco-2 cell monolayer integrity. Under conditions of incubation with M90T-SIgAC5, the TER was still at 70% of its original value at 24 h and dropped to 200 Ω/cm^2 after 40 h of incubation (not shown). Together, these data argue for the functional superiority of SIgA in retarding IEC infection from the apical pole and suggest that the mere presence of SIgAC5 MAb with a single specificity contributes to time-dependent, yet time-limited protection. In addition to unraveling the unique properties of a specific SIgA MAb to preserve Caco-2 cell integrity, these results demonstrate that the entry of *S. flexneri* is not restricted to the basolateral pole of IECs, in contradiction to the study of Mounier et al. (6). Various adjustments in the experimental settings, including the period of differentiation of epithelial cells on Transwell membranes, may justify such subtle differences and changes in the paradigm of the mode of infection of *S. flexneri*.

As *S. flexneri* is a nonmotile bacterium, the bacterial loads present in the cell lysates reflect the ability of the apically inoculated bacteria to adhere and infect cells. Following contact with IECs, capture of *S. flexneri* is a very rapid process (15 min) that necessitates the functional assembly of the T3SS for subsequent invasion (8). As our data (Fig. 1A) show that SIgAC5 is capable of delaying damage to polarized Caco-2 cell monolayers and that binding of pIgAC5 to *S. flexneri* results in the transient suppression of the T3SS proteins (18), we speculated that one of the functions of the MAb would be to inhibit either the binding to or/and the entry into IECs. Following overnight incubation, a marked reduction in the bacterial counts of whole-Caco-2 cell lysates was observed in the presence of SIgAC5 (Fig. 1B), whereas incubation with the other control MAbs yielded values similar to those of Caco-2 cells infected with the bacteria only (Fig. 1B). Upon treatment with gentamicin to eliminate surface-bound bacteria, the lysates of Caco-2 cells exposed to M90T-SIgAC5 (Fig. 1C) contained very low counts, suggesting that entry was efficiently inhibited, in agreement with MAb-mediated reduced attachment, a mechanism ensured by immune exclusion. Similar to TER values, these differences leveled off with increased incubation times (not shown), in support of the transient inhibition of the T3SS ensured by SIgAC5. Consistent with the lack of effect observed in the absence of antibiotic, the levels of internalized M90T in the presence of other MAbs resembled that of bacteria alone (Fig. 1C). Of note, translocated bacteria accumulated in the bottom of the wells of the basolateral compartment, preventing a potential cross-infection of the monolayers from the basolateral pole receptors for *S. flexneri* (4).

Diminished bacterial growth as a consequence of SIgAC5-mediated agglutination. In comparison with IgGC20 and monomeric IgAC5 (mIgAC5) with the same specificity, SIgAC5 proved to differentially protect the Caco-2 cell monolayer by more efficiently inhibiting *S. flexneri* attachment and entry. The avidity of polymeric IgA was shown to justify such an isotype- and molecular form-dependent difference in neutralizing *Clostridium difficile* toxin A (30). We hypothesized that in the context of a bacterium, additional features of SIgA, including its effect on bacterial growth and masking in large immune complexes, may explain its better functionality. As mentioned above, pIgAC5 suppresses the T3SS proteins and diminishes the biosynthesis of ATP (18); we therefore tested whether this can affect bacterial growth in solution as a function of time. Using the same bacterium-to-MAb ratio as in

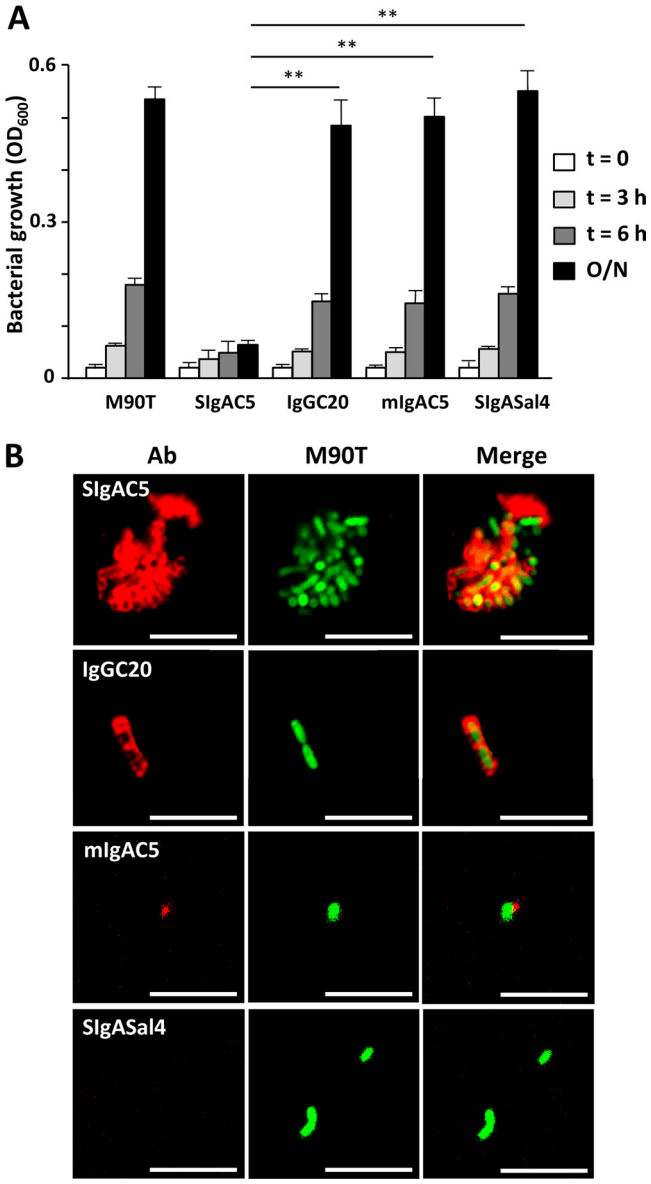

FIG 2 Bacterial agglutination occurs in the presence of LPS-specific SIgAC5 MAb only. (A) Growth of *S. flexneri* alone or in the presence of various MAbs as a function of time. Mean values + SEM are shown. Statistical differences are shown for the overnight (O/N) condition. OD_{600}, optical density at 600 nm. **, $P \leq 0.01$. (B) M90T expressing GFP was incubated with SIgAC5, IgGC20, monomeric IgAC5 (mIgAC5), and SIgASal4 stained with α chain- or γ chain-specific Abs and visualized by LSCM. Bacteria agglutinate only in the presence of SIgAC5, which contributes to the formation of immune complexes, resulting in large aggregates. Only surface coating (IgGC20 and mIgAC5) or no binding (SIgASal4) was observed with control MAbs. One representative field, obtained from 10 different observations following analysis of 3 different slides, is shown. Scale bars, 5 μm.

the experiments whose results are depicted in Figure 1, we found that a 3-h incubation with SIgAC5 reduced the bacterial counts by a factor of 1.4 compared with the results using M90T alone, while equimolar amounts of IgGC20, monomeric IgAC5, and SIgASal4 MAbs had no effect (Fig. 2A). In addition to the effect on bacterial growth, we found that aggregates formed within 1 h in the presence of tetravalent SIgAC5 only but not upon incubation with divalent specific IgGC20 or monomeric IgAC5 or nonspecific SIgASal4 of identical structure (Fig. 2B). At 6 h, only cells incubated with M90T-SIgAC5 exhibited a 2-fold reduction in bacterial counts in comparison with the counts in cells incubated with the bacteria grown alone or with the other MAbs, an effect that amplified further (up to 9-fold decrease) after overnight incubation (Fig. 2A). This strongly suggests that the impact on *S. flexneri* proliferation can account for reduced infection.

In agreement with the tetrameric valence of SIgAC5, the red-labeled MAb was present all over the opsonized lattice of M90T; in comparison, with IgGC20 and mIgAC5, the coating was limited to the surface of individual bacteria and no binding was detected for SIgASal4 (Fig. 2B). A similar pattern of immune complexes were still seen after overnight culture (data not shown), together with low levels of single bacteria, suggesting that a limited number of bacteria can escape SIgA-mediated agglutination over time. The agglutination-based capacity of anti-LPS-specific SIgAC5 to reduce binding to IECs, combined with its negative impact on *S. flexneri* growth, explains molecularly why SIgA exhibits protective functions toward sensitive IECs that are superior to those of the other MAbs tested.

SIgAC5 controls disruption of the Caco-2 cell monolayer by limiting the sites of productive infection. While the agglutination properties of SIgAC5 can justify its effect on bacteria, the beneficial impact on target IECs infected from the apical pole remains to be understood. The preserved TER and low bacterial counts (Fig. 1) strongly suggest that the neutralizing function of SIgA makes it more difficult for M90T to invade Caco-2 cells and allows the maintenance of the IEC monolayer integrity for a prolonged period. We thus analyzed quantitatively the beneficial protective role of SIgAC5 in comparison with the effects of other MAbs using LSCM images from whole Transwell filters (Fig. 3A and B). Incubation with M90T-SIgAC5 was the sole experimental condition to display a significant reduction in both the overall infected area and the number of infection foci after overnight exposure to polarized Caco-2 cell monolayers compared to the results for incubation with M90T alone and M90T in complex with the other MAbs tested. Upon analysis of LSCM images reflecting the representative pattern of each experimental condition, we found that surface-bound bacteria were neutralized by the SIgAC5 MAb only, while unlimited spreading occurred all over the monolayers in the other scenarios (Fig. 3C). SIgAC5 also drastically limited the expansion of infected foci and the development of large areas devoid of cells, as was observed with M90T alone or in complex with the other MAbs (Fig. 3C). Taken together, these results suggest that the agglutinating features of SIgAC5 restrict bacterial dissemination among neighbor cells (Fig. 3C), further supporting the concept that SIgA Abs elicited upon primary M90T infection are important in protecting against IEC reinfection and that this occurs by ensuring morphological integrity.

SIgAC5 delays destruction of the tight junction network and actin-based cell architecture. The data shown in Figure 3C suggest that IECs infected with *S. flexneri* undergo important structural changes, as revealed by the disappearance of the tight junction network and formation of areas devoid of cells. Within hours postinfection, the architecture of actin fibers changed drastically only in the periphery of the sites of interaction with M90T, supporting the idea that rearrangement of the cytoskeleton is induced by virulence factors expressed by the invading bacteria (Fig. 4A, arrowheads). Actin remodeling would aim at preventing excessive

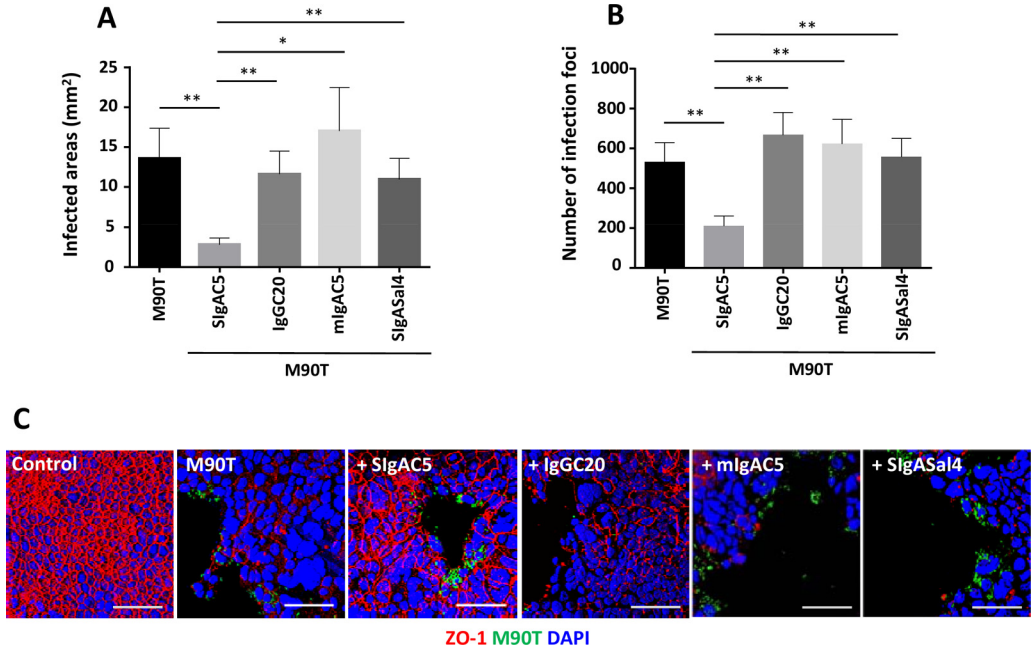

FIG 3 SIgA maintains Caco-2 cell monolayer integrity and limits M90T cellular dissemination. Damage inflicted on Caco-2 cell monolayers by apical addition of M90T alone or combined with various MAbs after overnight incubation was determined by measuring the sum of infected areas (A) and the number of infection foci (B) from LSCM images using ImageJ software. Data are expressed on a per-filter basis. Mean values + SEM are shown; $n = 3$ experiments carried out in triplicates. Statistically significant differences calculated by comparison with M90T-SIgAC5 are indicated above the columns as follows: **, $P \leq 0.01$; *, $P \leq 0.05$. (C) LSCM 3-dimensional reconstructed images (snapshot) of Caco-2 cell monolayers exposed overnight to M90T alone or in combination with various MAbs. Limited dissemination of bacteria (green) and maintenance of tight junctions stabilizing the monolayer (ZO-1 red labeling) was visualized with SIgAC5 only, while tight junction disappearance induced by uncontrolled infection is observed for all other experimental conditions. Caco-2 cell nuclei were stained with DAPI (blue). One representative field obtained from the observation of whole Transwell filters recovered from 3 experiments performed in triplicates is shown. Scale bars, 50 μm.

cellular damage during intracellular bacterial proliferation, allowing transient maintenance of local cohesion (ZO-1 distribution is preserved), a stratagem most likely achieved by the recently described OspE virulence factor (31, 32). The loss of the ZO-1 signal after overnight incubation reflects the beginning of the destruction of intercellular junctions (Fig. 4B) and is accompanied by the disappearance of the cell architecture, as mapped by the complete extinction of phalloidin detection. The *S. flexneri*-induced loss of the tight junction network and actin fiber depolymerization suggest a novel mode of invasion from the apical surface which promotes rapid bacterial propagation and dissemination within the monolayers, a process that may synergize with bacteria invading from the basolateral pole after M cell-mediated entry.

In sharp contrast, the aggregation mediated by SIgAC5 re-

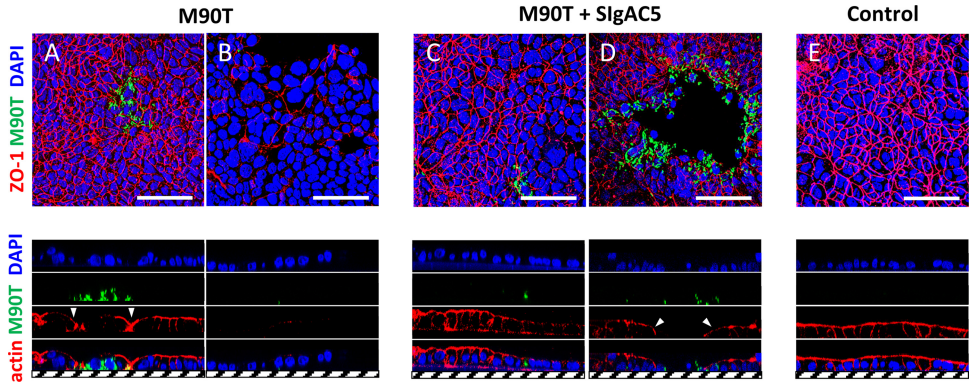

FIG 4 SIgA-mediated protection delays the disruption of tight junctions and depolymerization of actin fibers. LSCM 3-dimensional reconstructed images (snapshot) of Caco-2 cell monolayers exposed to M90T alone or in combination with SIgAC5 are shown; views are from the top (top panels) and along the ZX plan (bottom panels). (A) Invasive M90T (green) located intracellularly triggers actin remodeling at 10 h, as tracked by phalloidin staining (red, bottom panels). (B) Destruction of tight junctions (red, top panel) occurs 6 h later. (C) Limited infection in the presence of SIgAC5 prevents destruction of tight junctions and organized actin fibers. (D) Neutralization by the Ab results in delayed damage after overnight exposure. (E) Noninfected Caco-2 cell monolayers are depicted for comparison. The basal side of the Caco-2 cell monolayer is displayed as hatching on the bottom images. Sites of extensive actin remodeling are pinpointed by white arrowheads. Images are one example of 90 observed among 3 filters prepared from 3 independent experiments performed in triplicates. Scale bars, 50 μm.

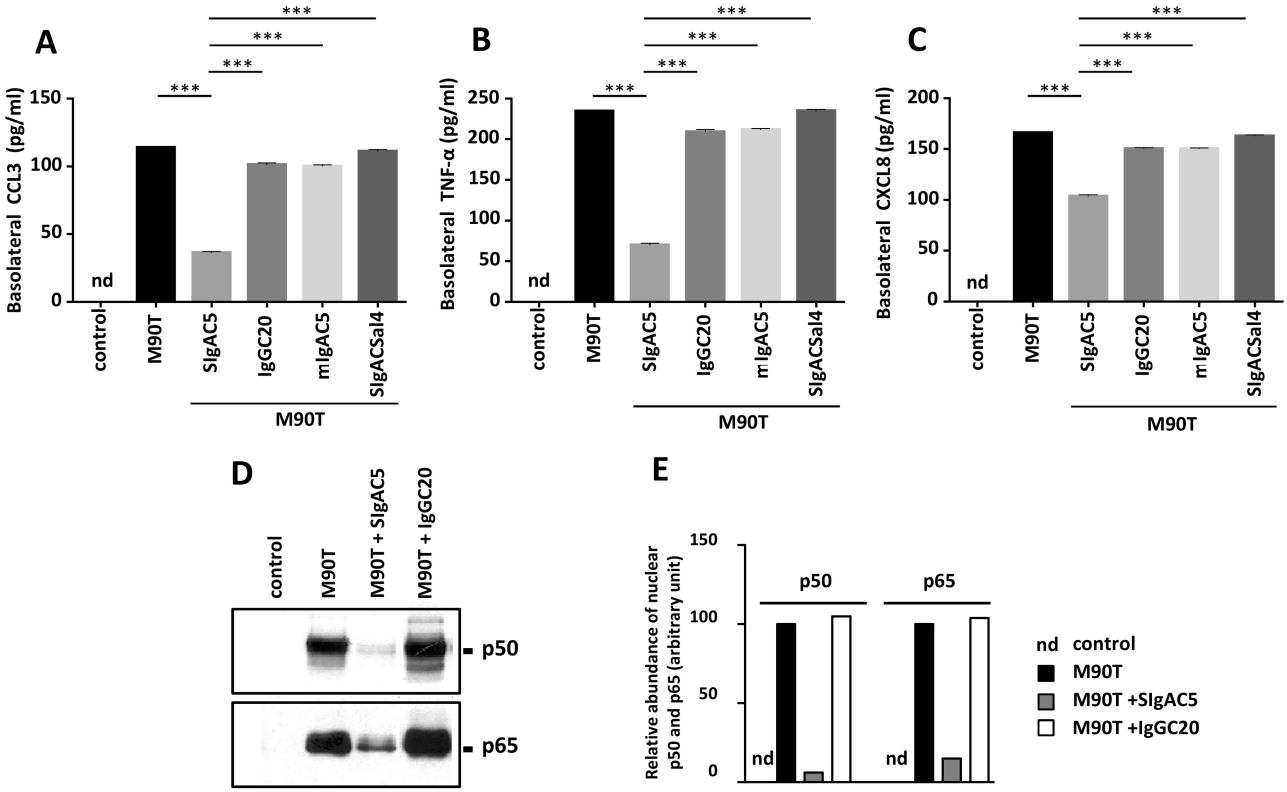

FIG 5 Anti-inflammatory properties of SIgA reduce secretion of proinflammatory mediators by polarized Caco-2 cell monolayers through inhibition of NF-κB nuclear translocation. Production of CCL3 (A), TNF-α (B), and CXCL8 (C) was measured in the basolateral compartment of Caco-2 cell monolayers incubated under various conditions after overnight incubation. Mean values + SEM are shown; $n = 3$ experiments in triplicate. ***, $P \leq 0.001$. (D) Immunoblotting of the NF-κB subunits p50 and p65/RelA in the nuclear extracts from Caco-2 cell monolayers apically incubated overnight with M90T alone or in complex with LPS-specific SIgAC5 and IgGC20 as a control. Panels are representative of one individual experiment performed in triplicate ($n = 3$). (E) Densitometric analysis of immunoblots described for panel D, exposed for optimal times to avoid saturation of the photographic film. The intensity of the signal reached with M90T alone was fixed at 100%. nd, not detectable.

sulted in punctate surface binding and prevented bacterial spreading, thus ensuring limited damage to a few targeted epithelial cells (Fig. 4C and D). Strikingly, outside the infected foci and despite a slight decrease in the detection of pericellular ZO-1 and organized actin fibers, exposure of Caco-2 cells to M90T-SIgAC5 overnight resulted in patterns similar to those in uninfected filters (Fig. 4D and E). Similar control experiments performed with M90T-IgGC20 revealed infection patterns similar to those observed for M90T alone (not shown).

SIgAC5 represses CCL3, TNF-α, and CXCL8 secretion by IECs via blocking of NF-κB nuclear translocation. We next hypothesized that the neutralizing ability of SIgAC5 would result in moderate apical sensing of the M90T strain by polarized Caco-2 cell monolayers. The production of CCL3 (macrophage inflammatory protein-1α), TNF-α, and CXCL8 (interleukin-8 [IL-8]) in the basolateral compartment, as well as the nuclear translocation of NF-κB, known to regulate the expression of the three mediators, were examined as markers of the Caco-2 cell proinflammatory response (5, 11, 33). SIgAC5 interacting with the M90T strain significantly reduced the production of CCL3 (≈70%), TNF-α (≈70%), and CXCL8 (≈35%) by Caco-2 cells compared with the levels obtained by incubation with M90T alone or in complex with the other MAbs tested (Fig. 5A, B, and C). This reflects in IECs the situation observed in the rabbit model, in which the expression of proinflammatory mediators in the Peyer's patch tissue is quenched when *S. flexneri* is administered as a complex with SIgAC5 (13). High nuclear translocation of the transcription factor NF-κB subunits p50 and p65 occurred after incubation with M90T alone or in complex with specific IgGC20 (Fig. 5D and E), whereas the exposure of Caco-2 cells to SIgAC5-based immune complexes led to a marked drop in the nuclear detection of either NF-κB subunit (Fig. 5D and E). The data reveal the prominent role of neutralizing extracellular SIgA in controlling the onset of cellular proinflammatory responses (7), a feature that contributes to maintaining the physical integrity of the epithelial barrier.

DISCUSSION

The functions of SIgA at mucosal surfaces are manifold, extending from transport of immune complexes across PPs, control of inflammatory circuits, intracellular neutralization of invading pathogens, and regulation of the microbiota to classical/paradigm immune exclusion (34). Despite the *in vivo* and *in vitro* demonstration of the importance of SIgA in the latter process, it remains unclear by which underlying mechanisms extracellular SIgA capable of preventing invasion can maintain short-range epithelial integrity. The results of the present study demonstrate that agglutinating SIgA precludes contact of the enteropathogen *S. flexneri* with target IECs, resulting in maintenance of tight junctions and

cell morphology and silencing of cellular proinflammatory pathways. Remarkably, this occurs in the absence of other immune partners usually involved in combating *S. flexneri* infection. Furthermore, the lack of mucus, known to contribute to repelling bacteria (35) and anchoring SIgA for improved functionality (36), does not negate the crucial role of SIgA in ensuring prolonged preservation of the polarized IEC monolayer. Similarly to SIgA-controlled entry of immune complexes through PPs, our data pave the way to exploring whether selective entry into IECs via CD71 (37) may contribute to the modulation of immune reactions, for example, allergy or gut inflammation.

It has been shown that the association of pIgAC5 with *S. flexneri* de-energized the T3SS by affecting the proton motive force and reducing cellular levels of ATP (18). Temporary incapacity of the bacterium to invade epithelial cells was suggested yet not experimentally tackled. Our results indicate that perturbation of the bacterial bioenergetics by SIgAC5-mediated agglutination leads to decreased growth rate, and this translates into delayed invasion of IECs compared to the time to invade their uncoated counterparts. Inhibition of other bacterial functions by IgA, i.e., motility, ultimately affecting bacterial entry into IECs has been reported for *Salmonella enterica* (38). Interestingly, masking of LPS and adhesins by Ab coating is not sufficient to disarm *S. flexneri*, as IgGC20 does not interfere with IEC invasion; this suggests that the lattice formed by bound SIgA may trigger mechanical constraints on the bacterial wall (39), leading to metabolic alterations not seen with monomeric IgA or IgG. This is reflected by the unique property of SIgAC5 to significantly lower the levels of CCL-3, TNF-α, and CXCL8 secreted by IECs when bound to *S. flexneri* in immune complexes. Reduced epithelial secretions due to SIgA-neutralized *S. flexneri* would be indicative of the ongoing immune response, with downregulation of proinflammatory signaling (13).

Another finding of our work resides in the observation that an LPS-specific SIgA MAb, but not IgA or IgG MAbs of the same specificity, inhibits the sequential lesions induced by luminal application of the virulent *S. flexneri* M90T strain in an intestinal epithelium model. The experimental setting was designed to study the effect of M90T-triggered damage after overnight infection, well beyond the time course usually accessible in *in vivo* models (13, 22). Bacteria were initially found to infect a limited number of polarized cells, leading to preferential targeting of the tight junction's seal; such a feature has been described for *S. flexneri* serotype 2 and also for other pathogens, such as enterohemorrhagic *Escherichia coli* and *Salmonella* strains (8, 9, 39), yet at very high MOI that do not reflect the low doses sufficient to infect the human gut. Over time, the progressive overwhelming proliferation of *S. flexneri* induced irreversible damage to the cell architecture, as reflected by the complete depolymerization of actin fibers. Loss of epithelial integrity is a well-accepted consequence of bacillary dysentery (40), and it appears to be mimicked in the *in vitro* model after bacterial exposure limited to the apical epithelial cell surface.

In vitro dissection turned out to be appropriate to evaluate the multilevel neutralizing properties of SIgAC5 directed against LPS from *S. flexneri*, as reflected in the delay of infection via mechanisms that included blocking of interaction with IEC monolayers, the reduction of bacterial growth and proliferation inside polarized Caco-2 cells, maintenance of the tight junction network, slowing down of actin fiber depolymerization, and interference with the activation of proinflammatory gene products, a sum of properties that can be assigned to the agglutinating characteristics of the SIgAC5 Ab isotype. Indeed, the combination of M90T with an LPS-specific IgGC20 and mIgAC5 MAb resulted in the same pattern of sequential IEC destruction as observed with M90T alone. However, following parenteral vaccination with O-specific polysaccharide 2a, transudating polyclonal IgG was found to protect the vaccinees (41), suggesting that multiple mechanisms staggered over time may be involved. In the absence of other levels of immune protection, this work sheds light on the functional role of luminal SIgA in interfering with infection by *S. flexneri* from the apical surface. This also suggests that by interfering with the very first and destructive steps of infection, LPS-specific SIgA must be considered an asset in the battery of molecular and cellular agents required in immunity against *S. flexneri*.

ACKNOWLEDGMENTS

This work was supported by Swiss Science Research Foundation grant no. 3100-138422.

We thank the laboratory of P. Sansonetti, Pasteur Institute, Paris, for providing bacterial strains and stimulating discussions.

REFERENCES

1. **Sansonetti PJ.** 2006. The bacterial weaponry: lessons from Shigella. Ann. N. Y. Acad. Sci. **1072:**307–312.
2. **Wassef JS, Keren DF, Mailloux JL.** 1989. Role of M cells in initial antigen uptake and in ulcer formation in the rabbit intestinal loop model of shigellosis. Infect. Immun. **57:**858–863.
3. **Zychlinsky A, Prevost MC, Sansonetti PJ.** 1992. Shigella flexneri induces apoptosis in infected macrophages. Nature **358:**167–169.
4. **Phalipon A, Sansonetti PJ.** 1999. Microbial-host interactions at mucosal sites. Host response to pathogenic bacteria at mucosal sites. Curr. Top. Microbiol. Immunol. **236:**163–189.
5. **Fernandez MI, Pedron T, Tournebize R, Olivo-Marin JC, Sansonetti PJ, Phalipon A.** 2003. Anti-inflammatory role for intracellular dimeric immunoglobulin A by neutralization of lipopolysaccharide in epithelial cells. Immunity **18:**739–749.
6. **Mounier J, Vasselon T, Hellio R, Lesourd M, Sansonetti PJ.** 1992. Shigella flexneri enters human colonic Caco-2 epithelial cells through the basolateral pole. Infect. Immun. **60:**237–248.
7. **Perdomo OJ, Cavaillon JM, Huerre M, Ohayon H, Gounon P, Sansonetti PJ.** 1994. Acute inflammation causes epithelial invasion and mucosal destruction in experimental shigellosis. J. Exp. Med. **180:**1307–1319.
8. **Romero S, Grompone G, Carayol N, Mounier J, Guadagnini S, Prevost MC, Sansonetti PJ, Van Nhieu GT.** 2011. ATP-mediated Erk1/2 activation stimulates bacterial capture by filopodia, which precedes Shigella invasion of epithelial cells. Cell Host Microbe **9:**508–519.
9. **Sakaguchi T, Kohler H, Gu X, McCormick BA, Reinecker HC.** 2002. Shigella flexneri regulates tight junction-associated proteins in human intestinal epithelial cells. Cell. Microbiol. **4:**367–381.
10. **Le-Barillec K, Magalhaes JG, Corcuff E, Thuizat A, Sansonetti PJ, Phalipon A, Di Santo JP.** 2005. Roles for T and NK cells in the innate immune response to Shigella flexneri. J. Immunol. **175:**1735–1740.
11. **Sansonetti PJ, Arondel J, Huerre M, Harada A, Matsushima K.** 1999. Interleukin-8 controls bacterial transepithelial translocation at the cost of epithelial destruction in experimental shigellosis. Infect. Immun. **67:**1471–1480.
12. **Schultsz C, Qadri F, Hossain SA, Ahmed F, Ciznar I.** 1992. Shigella-specific IgA in saliva of children with bacillary dysentery. FEMS Microbiol. Immunol. **4:**65–72.
13. **Boullier S, Tanguy M, Kadaoui KA, Caubet C, Sansonetti P, Corthésy B, Phalipon A.** 2009. Secretory IgA-mediated neutralization of Shigella flexneri prevents intestinal tissue destruction by down-regulating inflammatory circuits. J. Immunol. **183:**5879–5885.
14. **Cohen D, Block C, Green MS, Lowell G, Ofek I.** 1989. Immunoglobulin M, A, and G antibody response to lipopolysaccharide O antigen in symptomatic and asymptomatic Shigella infections. J. Clin. Microbiol. **27:**162–167.
15. **Islam D, Veress B, Bardhan PK, Lindberg AA, Christensson B.** 1997. Quantitative assessment of IgG and IgA subclass producing cells in rectal mucosa during shigellosis. J. Clin. Pathol. **50:**513–520.

16. **Phalipon A, Michetti P, Kaufmann M, Cavaillon JM, Huerre M, Kraehenbuhl JP, Sansonetti PJ.** 1994. Protection against invasion of the mouse pulmonary epithelium by a monoclonal IgA directed against Shigella flexneri lipopolysaccharide. Ann. N. Y. Acad. Sci. **730:**356–358.
17. **Rasolofo-Razanamparany V, Cassel-Beraud AM, Roux J, Sansonetti PJ, Phalipon A.** 2001. Predominance of serotype-specific mucosal antibody response in Shigella flexneri-infected humans living in an area of endemicity. Infect. Immun. **69:**5230–5234.
18. **Forbes SJ, Bumpus T, McCarthy EA, Corthésy B, Mantis NJ.** 2011. Transient suppression of Shigella flexneri type 3 secretion by a protective O-antigen-specific monoclonal IgA. mBio **2:**00042–11. doi:10.1128/mBio.00042-11.
19. **Thierry AC, Bernasconi E, Mercenier A, Corthésy B.** 2009. Conditioned polarized Caco-2 cell monolayers allow to discriminate for the ability of gut-derived microorganisms to modulate permeability and antigen-induced basophil degranulation. Clin. Exp. Allergy **39:**527–536.
20. **Rathman M, Jouirhi N, Allaoui A, Sansonetti P, Parsot C, Tran Van Nhieu G.** 2000. The development of a FACS-based strategy for the isolation of Shigella flexneri mutants that are deficient in intercellular spread. Mol. Microbiol. **35:**974–990.
21. **Kadaoui KA, Corthésy B.** 2007. Secretory IgA mediates bacterial translocation to dendritic cells in mouse Peyer's patches with restriction to mucosal compartment. J. Immunol. **179:**7751–7757.
22. **Phalipon A, Kaufmann M, Michetti P, Cavaillon JM, Huerre M, Sansonetti P, Kraehenbuhl JP.** 1995. Monoclonal immunoglobulin A antibody directed against serotype-specific epitope of Shigella flexneri lipopolysaccharide protects against murine experimental shigellosis. J. Exp. Med. **182:**769–778.
23. **Phalipon A, Costachel C, Grandjean C, Thuizat A, Guerreiro C, Tanguy M, Nato F, Vulliez-Le Normand B, Bélot F, Wright K, Marcel-Peyre V, Sansonetti PJ, Mulard LA.** 2006. Characterization of functional oligosaccharide mimics of the Shigella flexneri serotype 2a O-antigen: implications for the development of a chemically defined glycoconjugate vaccine. J. Immunol. **176:**1686–1694.
24. **Michetti P, Mahan MJ, Slauch JM, Mekalanos JJ, Neutra MR.** 1992. Monoclonal secretory immunoglobulin A protects mice against oral challenge with the invasive pathogen Salmonella typhimurium. Infect. Immun. **60:**1786–1792.
25. **Favre LI, Spertini F, Corthésy B.** 2003. Simplified procedure to recover recombinant antigenized secretory IgA to be used as a vaccine vector. J. Chromatogr. B Analyt. Technol. Biomed. Life Sci. **786:**143–151.
26. **Crottet P, Cottet S, Corthésy B.** 1999. Expression, purification and biochemical characterization of recombinant murine secretory component: a novel tool in mucosal immunology. Biochem. J. **341:**299–306.
27. **Crottet P, Corthésy B.** 1998. Secretory component delays the conversion of secretory IgA into antigen-binding competent F(ab′)2: a possible implication for mucosal defense. J. Immunol. **161:**5445–5453.
28. **Cottet S, Corthésy-Theulaz I, Spertini F, Corthésy B.** 2002. Microaerophilic conditions permit to mimic in vitro events occurring during in vivo Helicobacter pylori infection and to identify Rho/Ras-associated proteins in cellular signaling. J. Biol. Chem. **277:**33978–33986.
29. **Sansonetti PJ, Kopecko DJ, Formal SB.** 1982. Involvement of a plasmid in the invasive ability of Shigella flexneri. Infect. Immun. **35:**852–860.
30. **Stubbe H, Berdoz J, Kraehenbuhl JP, Corthésy B.** 2000. Polymeric IgA is superior to monomeric IgA and IgG carrying the same variable domain in preventing Clostridium difficile toxin A damaging of T84 monolayers. J. Immunol. **164:**1952–1960.
31. **Kim M, Ogawa M, Fujita Y, Yoshikawa Y, Nagai T, Koyama T, Nagai S, Lange A, Fässler R, Sasakawa C.** 2009. Bacteria hijack integrin-linked kinase to stabilize focal adhesions and block cell detachment. Nature **459:**578–582.
32. **Kim M, Ogawa M, Mimuro H, Sasakawa C.** 2010. Reinforcement of epithelial cell adhesion to basement membrane by a bacterial pathogen as a new infectious stratagem. Virulence **1:**52–55.
33. **Pedron T, Thibault C, Sansonetti PJ.** 2003. The invasive phenotype of Shigella flexneri directs a distinct gene expression pattern in the human intestinal epithelial cell line Caco-2. J. Biol. Chem. **278:**33878–33886.
34. **Mantis NJ, Rol N, Corthésy B.** 2011. Secretory IgA's complex roles in immunity and mucosal homeostasis in the gut. Mucosal Immunol. **4:**603–611.
35. **Johansson ME, Phillipson M, Petersson J, Velcich A, Holm L, Hansson GC.** 2008. The inner of the two Muc2 mucin-dependent mucus layers in colon is devoid of bacteria. Proc. Natl. Acad. Sci. U. S. A. **105:**15064–15069.
36. **Corthésy B.** 2010. Role of secretory immunoglobulin A and secretory component in the protection of mucosal surfaces. Future Microbiol. **5:**817–829.
37. **Lebreton C, Ménard S, Abed J, Moura IC, Coppo R, Dugave C, Monteiro RC, Fricot A, Traore MG, Griffin M, Cellier C, Malamut G, Cerf-Bensussan N, Heyman M.** 2012. Interactions among secretory immunoglobulin A, CD71, and transglutaminase-2 affect permeability of intestinal epithelial cells to gliadin peptides. Gastroenterology **143:**698–707.
38. **Forbes SJ, Eschmann M, Mantis NJ.** 2008. Inhibition of Salmonella enterica serovar Typhimurium motility and entry into epithelial cells by a protective antilipopolysaccharide monoclonal immunoglobulin A antibody. Infect. Immun. **76:**4137–4144.
39. **Horejs C, Ristl R, Tscheliessnig R, Sleytr UB, Pum D.** 2011. Single-molecule force spectroscopy reveals the individual mechanical unfolding pathways of a surface layer protein. J. Biol. Chem. **286:**27416–27424.
40. **Guttman JA, Finlay BB.** 2009. Tight junctions as targets of infectious agents. Biochim. Biophys. Acta **1788:**832–841.
41. **Phalipon A, Tanguy M, Grandjean C, Guerreiro C, Bélot F, Cohen D, Sansonetti PJ, Mulard LA.** 2009. A synthetic carbohydrate-protein conjugate vaccine candidate against Shigella flexneri 2a infection. J. Immunol. **182:**2241–2247.